Supplementary Information for

A Genetic History of Continuity and Mobility in the Iron Age Central Mediterranean

Hannah M. Moots, Margaret Antonio, Susanna Sawyer, Jeffrey P. Spence, Victoria Oberreiter, Clemens L. Weiß, Michaela Lucci, Mehdi Cherifi, Francesco La Pastina, Francesco Genchi, Elisa Praxmeier, Brina Zagorc, Olivia Cheronot, Kadir T. Özdoğan, Lea Demetz, Selma Amrani, Francesca Candilio, Daniela De Angelis, Gabriella Gasperetti, Daniel Fernandes, Ziyue Gao, Mounir Fantar, Alfredo Coppa, Jonathan K. Pritchard*, Ron Pinhasi*

*Corresponding authors
Email: pritch@stanford.edu (J.K.P.); ron.pinhasi@univie.ac.at (R.P.)

This PDF file includes:

Table of Contents

Supplementary Text
Site descriptions
Kerkouane
Geographical coordinates: 36.9615, 11.0804
Analyzed individuals: R11749, R11751, R11776, R11746, R11790, R11793, R11753, R11755, R11759, R11778, R11780, R11791
Date range of individuals reported in this study: 761 - 250 cal BCE

Kerkouane is an exceptionally well-preserved Punic town located on Tunisia's Cap Bon Peninsula and provides one of the best-surviving windows into Carthaginian daily life (1–4). Due to the destruction of Carthage and many of its territories at the end of the Punic Wars, as well as the continued use and development or rebuilding of these towns under Roman control, insights into Carthaginian daily life are limited.

Originally inhabited from 650 - 250 BCE, the population of Kerkouane is thought to have been around 1,200 with an economy primarily based on the production and export of marine resources from the region, including the production and exportation of garum, salt, and the eponymous purple dye derived from locally harvested Murex sp. shells (5). Kerkouane was abandoned after the 1st Punic War between Carthage and Rome and was never re-inhabited or rebuilt by the Romans resulting in the excellent preservation of the original Punic architecture of the town.

Sant'Imbenia
Geographical coordinates: 40.5938, 8.2045
Analyzed individuals: R11828, R11829, R11835
Date range of individuals reported in this study: 1115 - 774 cal BCE

The archaeological site of Sant'Imbenia lies in Porto Conte Bay, a natural harbor called Portus Nympharum by the geographer Ptolemy in the second century AD, 10 km to the WNW of Alghero (SS). During the fourteenth century BCE, a single-tower nuraghe was built at Sant'Imbenia, surrounded by huts within the current coastline, and subsequently surrounded by a bastion (6, 7). The nuraghe was in use until the tenth century BCE and the village evolved towards an "urban" organization at the end of the ninth century BCE, around an open space interpreted as a market square. This development is related to seafaring travels around the Western Mediterranean Sea by Phoenicians, Etruscans and Greeks. The site remained a very active center at least until the seventh century BCE, an era of transformations in the indigenous world, which saw the establishment of the Phoenician colonies in SW of Sardinia (8–10).

About 900 m SW of the nuragic village, between the first and third centuries CE was built and inhabited the seaside villa of Sant'Imbenia, a large private dwelling dedicated to holidaying and leisure, covering a total area of over 3500 m2, decorated with precious elements, mosaics and refined stucco work on the walls and ceiling, that testify to an opulent lifestyle, found only in Lazio, in Rome, and in the Campi Flegrei area in Campania. Archaeological stratigraphies show that it was still inhabited at least until the 7th century AD, no longer as a luxurious private residence, but sporadically by small social groups, simple pastoral and farming communities (11, 12).

An area used as a necropolis, dating back to I-III century AD, was identified and partially excavated in the 1960s near the road connecting the hamlet of Santa Maria la Palma to Porto Conte. Some burials reused limestone steles with schematically engraved human faces dated to Punic-roman age (13). Later, in 1990s, an emergency archaeological excavation due to the installation of a pipeline was directed by the Superintendence of Archaeological Heritage for the Provinces of Sassari and Nuoro, with the excavation

of other burials, mainly human graves, often within amphorae, and sometimes used for multiple burials.

The samples being analyzed come from a stratigraphy damaged by previous land drainage works, plowing and stone removal carried out during the twentieth century. For these reasons, for example, tombs 1, 2, 3, 4 were upset. The necropolis, extremely poor in dating materials, has been referred to the Roman imperial age; however we cannot exclude the presence of remains from a previous period, possibly in a secondary position, due to the conditions of the excavation.

Tarquinia
Geographical coordinates: 42.2542, 11.7576
Analyzed individuals: R10337, R10338, R10339, R10340, R10341, R10342, R10343, R10344, R10359, R10361, R10363
Date range of individuals reported in this study: 759 cal BCE - 3 cal CE

Tarquinia, for the Etruscans Tarchna, was one of the four major urban centers of southern Etruria. It can be traced back all the way to the very origins of the Etruscan people. Located 72 kilometers north of Rome, near the Tyrrhenian Sea coast, Tarquinia was inhabited throughout the Iron Age and served as one of the primary trading ports between Etruria and the civilizations of the Mediterranean. It's a happy coincidence that the archaeological record coincides with the mythological tale of the founding of the city. This was in the period defined as "Villanovan", the birth of the Etruscan people.

The complexity and richness of the finds that have come down to us from the Villanovan period are amazing. This is particularly true of the objects from the burial grounds of Arcatelle, Poggio Selciatello, Selciatello sopra, Le Rose and Villa Bruschi Falgari (6). Over the years these have been added to by the results from archaeological excavations and field surveys on the actual settlement sites, Civita, pianoro dei Monterozzi and Poggio Cretoncini (7, 8).

From the end of the ninth to the early eighth century BCE, Tarquinia can be seen, most of all, as a hub, between southern Etruria, southern Italy as a whole and Sardinia. There are also signs of it having become a leading light both culturally and in the political/cultural world. This culminated in what is known as the Orientalising period. Here there was a consolidated social stratification, with locally crafted merchandise on offer to a world that offered commercial and cultural links.

The port of Gravisca was founded at the end of the Orientalising period. It provided an opening to the Greek, North African and broader Mediterranean world. This was when Tarquinia's first funerary paintings appeared, such as the tomb of the leopards, shown in Fig. S13. This period was an exceptional season of painted tombs that graced Tarquinia from about 530 BCE almost nonstop until the Hellenistic period in the fourth to third century BCE. In total, over 6000 tombs have been identified at Tarquinia's Monterozzi necropolis. About 200 of these tombs include feature wall tombs depicting a range of scenes from Etruscan feasting, daily life, and mythology.

Tarquinia's role during the fifth century BCE was probably, in part, dulled by sumptuary laws and an internal socio-political transformation of the community. However, this didn't prevent it from taking part in the Etruscan dodecapolis, the union of the twelve major urban centers. Tarquinia went to war with Rome on more than one occasion, finally being undone at the battle of Sentino in 295 BCE (9).

Pian Sultano
Geographical coordinates: 42.0263, 11.9483
Analyzed individuals: R11102, R11104, R11105, R11107
Date range of individuals reported in this study: 2000 - 1600 BCE

The Bronze Age settlement of Pian Sultano is located in central Italy, near modern-day Cerveteri (the Etruscan town of Caere). The earliest record for settlement at the site dates to 2000 BCE. Archaeological investigations of the site have uncovered artifacts indicating Pian Sultano was a farming community that also drew heavily on marine resources. Many ceramics feature design motifs characteristic of the central Italy Apennine culture. Long-distance trade is also indicated in the material culture of the site by obsidian blades, the material for which would have been procured from one of the 4 central Mediterranean island sources - Lipari, Pantelleria, Sardinia, or Sicily (10).

Methods

Date determination and radiocarbon dating

To determine the chronological dates for the individuals in the study, AMS radiocarbon dating was conducted on 60% of the individuals. This includes all three individuals from Sant'Imbenia, 2 individuals from Pian Sultano, 6 individuals from Kerkaoune, and 7 individuals from Tarquinia. We made sure to send an aliquot from at least 1 individual per tomb so that we could obtain an estimate for the use dates of each tomb.

The aliquots sampled consisted of 1 gram of dense petrous bone. These were sent to the W.M. Keck Carbon Cycle Accelerator Mass Spectrometer Lab at the University of California at Irvine. The results were calibrated using the intCal20 calibration curve using the OxCal interface (https://c14.arch.ox.ac.uk/oxcal/OxCal.html). We report these results in Dataset S3.

For individuals not sent for dating, we report both the maximum date range obtained through radiocarbon dating of individuals from the same tomb as well as the archaeologically estimated dates and we used the widest date range available of the two. We made one exception to this for Tomb 6176 at Tarquinia, for which the radiocarbon dates and archaeologically estimated dates were discordant. While the archaeological date estimates place this tomb in the early Iron Age (1000 - 900 BCE), radiocarbon dating in the last two centuries BCE (160 BCE to 3 CE). For these individuals, we used the range of the radiocarbon dates individuals from the tomb.

Isotopic Analyses - Carbon and Nitrogen

Dietary isotopes (Carbon and Nitrogen) are informative of food sources a person consumed during their lifetime. We obtained dietary isotopic data for the same individuals submitted for radiocarbon dating at the W.M. Keck Carbon Cycle Accelerator Mass Spectrometer Lab. We report these results in Dataset S3.

Individuals at Kerkouane had high nitrogen isotope values, indicative of diets high in meat, especially marine sources of protein. Marine resources were an important part of the economy of Kerkouane, where Tyrian purple dye and garum were two of the town's major exports. Given its geographic location on Cap Bon Peninsula, Kerkouane also served as an important stop for ships on long-distance voyages across the Mediterranean. One individual, R11780, has very high nitrogen value compared to other individuals from the same site. Genetically this individually forms a clade in qpWave analysis with contemporaneous Sicilian and Greek individuals One possibility is that these values reflect the diet of someone who spent large parts of their life at sea, consuming marine resources.

The individuals at Sant'Imbenia have moderate meat/marine consumption, and those at Tarquinia have lower levels (Fig S11), although it should be cautioned that this cannot be interpreted as dietary differences across sites without a study of the isotopic values of flora and fauna from each site as well, to serve as a background for comparison.

DNA extraction and library preparation

We cleaned, isolated, and powdered the cochlear portion of the petrous bone in dedicated clean rooms following the protocols described in (11, 12). Using 50mg of bone powder, DNA was extracted by 18-hour incubation of the powder in a solution of Proteinase-K and EDTA. The DNA was then eluted in 50 µl 10 mM Tris-HCl, 1 mM EDTA, 0.05% Tween-20, pH 8.0 as in (13, 14).

Following a 30-minute uracil–DNA–glycosylase (UDG) treatment, double-stranded library preparation followed a modified version of the (15) protocol. Libraries were double-indexed with Accuprime Pfx Supermix. The PCR cycling conditions used were as follows: initial denaturation at 95°C for 5 min followed by 12 cycles of 95°C for 15 seconds, 60°C for 30 seconds, and 68°C for 30 seconds with a final elongation at 68°C for 5 min. After indexing, the libraries are purified using the MinElute system (Qiagen) and eluted in 25uL of 1 mM EDTA, 0.05% Tween-20.

Libraries passing screening based on DNA concentration were sequenced on an initial next-Seq screening run. Computational authentication of the presence of endogenous ancient DNA was based on 1) the presence of reads mapping to the human genome (hg19 assembly), 2) on the damage patterns at the terminal ends of reads, and 3) contamination analyses using Schmutzi (16), as done in (17).

We created and screened libraries from 23 Estrucan individuals (16 from the site of Tarquinia, 4 from Nepi Sante Grotte Gigliastro and 4 from Vulci Osteria), with 11 libraries (all from Tarquinia) passing the endogenous preservation and quality control measures described above. From Kerkouane, we created libraries for 20 individuals, with 12 successfully passing preservation and quality control standards. All libraries created for Sant'Imbenia (n=3) and Pain Sultano (n=4) successfully passed our screening thresholds.

Sequencing read processing and library screening

Libraries were sequenced on an Illumina NovaSeq 6000 sequencing platform to generate whole-genome shotgun data, with an average genome-wide coverage of 1.1x (range: 0.61 - 1.9x). Sequencing data was processed and pseudohaploid genotypes were called as done in (17), as summarized here. All libraries were initially sequenced to low coverage on using Illumina NovaSeqSP for screening of endogenous DNA preservation and authentication. Following demultiplexing, we used damage patterns to authenticate the libraries, with a minimum threshold of 5% deamination on the terminal ends of the reads. For subsequent analyses, 2 base-pairs were trimmed from the end of reads. The trimmed reads were then aligned to the human genome (hg19), filtered for quality, and deduplicated. Adapters were removed from libraries using Cutadapt (v1.14) (18). Reads were filtered for minimum length of 30, then aligned to hg19 using bwa (0.7.15-r1140) (19). For each library, aligned reads were sorted by coordinate using Picard's SortSam (version 2.9.0-1-gf5b9f50-SNAPSHOT) and read groups were added using Picard's AddOrReplaceReadGroups (version 2.9.0-1-gf5b9f50-SNAPSHOT) (http://broadinstitute.github.io/picard/). Reads with mapping quality < 25 (including unaligned reads) were filtered out. Duplicates were removed using samtools rmdup (http://www.htslib.org/doc/samtools.html) (20).

Genome-wide and chromosomal coverage were assessed using depth-cover (version 1.0.3, https://github.com/jalvz/depth-cover). Samples were screened and selected using the following criteria: 1) >10% reads aligned to the hg19 build of the human genome; 2) a C>T mismatch rate at the 5'-end and G>A at the 3'-end of the sequencing read of 5% or above (characterized with mapDamage v2.0.8) (21); 3) with a contamination level <= 3%. Contamination rates were estimated with three methods: 1) damage pattern and polymorphism in mitochondrial DNA with Schmutzi (16), 2) atypical ratios of coverages of X and Y chromosomes to autosomes calculated with ANGSD (22) and 3) for male samples, high heterozygosity on non-pseudo-autosomal region of the X chromosome with the "contamination" tool in ANGSD (22). Individual biological sex determination was inferred based on the ratio of reads from sex chromosomes and autosome coverages.

Calling pseudohaploid genotypes
Pseudohaploid genotypes for individuals in this study were called using the pipeline and tool created by Stephan Schiffels (https://github.com/stschiff/sequenceTools). Samtools mpileup was used to generate read coverage of a select SNP. For maximum overlap with published ancient and modern samples, variants were selected based on those used in the Human Origins panel and in the modern reference panel published by Lazaridis et. al. 2014 (23). This resulted in a total of 481,259 SNPs. A filter of minimum base and mapping quality of 30 (--min-BQ and --min-MQ) were also applied during samtools mpileup. Pseudohaploid genotypes were called by randomly choosing one allele from each site where there was read coverage, using pileupCaller.

Newly generated data merged with published data
In total, 30 individual genomes passed endogenous preservation and quality control thresholds (Fig. 2; Dataset S1). For the analyses in the paper, we merged the newly generated data reported here with the Allen Ancient DNA Resource v44 (49) using PLINK v1.9059. We also added recently published data from Bronze Age Italy to the reference dataset (17). We performed all subsequent analyses on autosomal data.

Inference of mitochondrial DNA haplogroups and contamination
Schmutzi (16) was used to estimate mitochondrial haplogroups and mitochondrial-based contamination estimates, as in (17). For determining mitochondrial contamination and the endogenous mitochondrial genome, we used untrimmed reads to identify and extract only reads with a damage signature. The endogenous consensus mitochondrial genome was called simultaneously while estimating mitochondrial contamination using schmutzi (16). Sequencing reads were aligned to the revised Cambridge Reference Sequence (rCRS) mitochondrial genome (NC_012920.1).

We used the contDeam tool in schmutzi with the following parameters: length of expected deamination set to 2 (--lengthDeam 2) and library type set to double strand (--library double). Schmutzi was used to 1) estimate contamination based on a haplogroup frequency database in tandem with the deamination estimates from contdeam and 2) to assemble the endogenous consensus mitochondrial genome informed by contamination. Base quality filtering of 30 (--qual 30) and the --uselength parameter were both used. This provided a contamination estimate based on deamination rates, a contamination estimate based on haplogroup frequencies, a contaminant mitochondrial genome, and an endogenous mitochondrial genome.

Haplogroups for the endogenous mitochondrial genomes were called using the command line version of Haplogrep (v2.1.20) (24). Contamination estimates are reported along with X chromosome contamination estimates, where possible (for males). Endogenous haplogroups and contamination estimates are reported in Dataset S1. Endogenous haplogroups are visualized in Fig. S11 and S12.

Kinship Determination
Kinship analysis was performed using READ (Relationship Estimation from Ancient DNA) (25). We identified one pair of related individuals, R11104 and R11105, consistent with a first-degree relationship (i.e. parent and cold). These two individuals were buried together in tomb 2 at the Bronze Age site of Pian Sultano, along with two other unrelated individuals. Genomic data for all 4 are reported in this study. Interestingly, although a number of individuals from the Iron Age sites (Table S1) were also interred in shared burials, none of these individuals were determined to be first- or second-degree biological kin.

Calculation of heterozygosity
We calculated heterozygosity using variants that are already known to be segregating in human populations, following the same approach as in (17). Three study samples, all from Iron Age Kerkouane (Tunisia), had heterozygosity beyond one standard deviation of the population average for that region. R11759, an individual with Saharan or sub-Saharan ancestry, has high heterozygosity. R11753 and R11791, have low heterozygosity (Fig. S9).

Runs of homozygosity
We followed the same approach as in (17) to estimate recent inbreeding by calculating runs of homozygosity (ROH). Only four samples had more than one ROH segment of 5Mb or longer (Table S2). Two individuals from Kerkouane, R11753 and R11791, show strong evidence of inbreeding, with ROH segments over 50Mb in length. In both cases, with over 12% of the genome being homozygous (segments > 5Mb in length), the parents were likely 2nd-degree relatives. Consistent with the homozygosity analysis, both individuals also have very low conditional heterozygosity (Fig. S9). While it is known that endogamous marriage practices were common in the contemporaneous ancient Greek world, less is known about such practices in the Carthaginian world, due to fewer surviving written records (26). The other two individuals with more than one ROH segment (R11778 and R10339) have little evidence of inbreeding as only less than 1% of their genome is homozygous.

Principal Component Analysis
We generated a Principal Component Analysis (PCA) reference space based on modern populations from around the Mediterranean, Europe, the Middle East, and North Africa using the tool smartpca from the EIGENSOFT package version 8.0.0 (27). The list of these modern populations and corresponding individual IDs can be found in Dataset S2. We project a set of ancient individuals, primarily from the Bronze and Iron Age Mediterranean, onto the modern reference space (Fig. 3, Fig. 4A). We used the parameter “numoutlieriter:0” to retain all outlier individuals in the projections, and “shrinkmode: YES” to correct for shrinkage towards the origin when estimating PC scores.

qpAdm and qpWave modeling
We carried out *qpAdm* and *qpWave* analyses using ADMIXTOOLS2 (28). ADMIXTOOLS2 uses F2 statistics as the basis for all downstream analysis. When computing F2s on this dataset, we used maxmiss = 0.5. For modeling the distal ancestries (shown in Fig. 4, S5), we used Mbuti.DG, Russia_Ust_Ishim.DG, CHG, Russia_EHG, Iberia_ElMiron, Czech_Vestonice1, Russia_MA1_HG.SG, Israel_Natufian, Jordan_PPNB as outgroup populations, referred to here as “Right Set A”. The IDs for each individual in each of these outgroup populations can be found in Dataset S2. For both qpAdm and qpWave, we used the default settings of ADMIXTOOLS2. ADMIXTOOLS2 automatically detects between diploid and pseudohaploid data. Since we are using pseudohaploid data, the program functions similar to the Admixtools, Inbreed=YES option.

We chose a set of distal source populations previously shown to be informative for understanding the diversity of the Mediterranean during this period for qpAdm admixture modeling, including Western Hunter-Gatherer (WHG), Yamnaya Samara, Anatolian Neolithic, Iranian Neolithic, and Late Neolithic farmers from Morocco, referred to here as “Left Set A” (17, 29, 30). To find the best fitting combinations of distal sources, we use qpadm_rotate() to compare all possible combinations of these source populations for each individual. In each iteration of the rotation, any of the potential source populations from Left Set A not used as sources in the model are added to the list of outgroup (right) populations. We then selected all models with a p-value greater than 0.5 with the fewest number of source populations. This could potentially be more than one model, and we indicated in figures and the text when this is the case. We

then ran qpAdm() on each working model to calculate the ancestry proportions, as well as standard errors.

For R11759, there were no working distal qpAdm models with the original set (Set B) of 5 distal source populations (Fig. 5). We replaced Morocco Late Neolithic with Morocco Early Neolithic farmers and a hunter-gatherer individual from Ethiopia from ~4500 BP, both of which produced working models. Using competition modeling (where possible sources are rotated to the outgroup), the best model uses ~70% Morocco Early Neolithic ancestry and ~30% Anatolia Neolithic (Fig. 4, Fig. S6).

We used the union of Right Set A and Left Set A as reference populations to perform pairwise qpWave on a set of Bronze and Iron Age individuals to test whether each individual in the pair can be modeled with the same ancestry components in qpAdm in comparison to a set of reference populations. Clustering was generated using 1 - log(p-value) to calculate distances between each individual, with clusters called by the cutree tool in R. This approach tests whether each pair of individuals can be modeled using the same ancestry components in qpAdm. This helps us identify groups of individuals from different geographic locations who can be modeled similarly. Given the genetic heterogeneity that characterizes the Iron Age Mediterranean, these groupings identified in qpWave help identify genetically similar individuals across regions.

ADMIXTURE modeling

We used supervised ADMIXTURE modeling to interpret the study individuals as a mixture of source populations (31). To determine the appropriate populations and number of populations to use as “sources” for supervised admixture, we performed unsupervised admixture for k = 2 through 7, with 5-fold cross validation, and 4 repetitions of each k. Runs for k = 3 through 5 had the lowest cross validation errors across repetitions. As a result of these runs, we selected 5 source populations that each maximized a unique component at k = 5 in the unsupervised run: Western Hunter-Gatherers (WHG), Anatolia Neolithic Farmers, Iranian Neolithic Farmers, Moroccan Hunter-Gatherer and Early Neolithic Farmers, Eneolithic Steppe Herders. A list of all individuals used to represent each population in the analyses can be found in Dataset S2.

Supplementary Figures

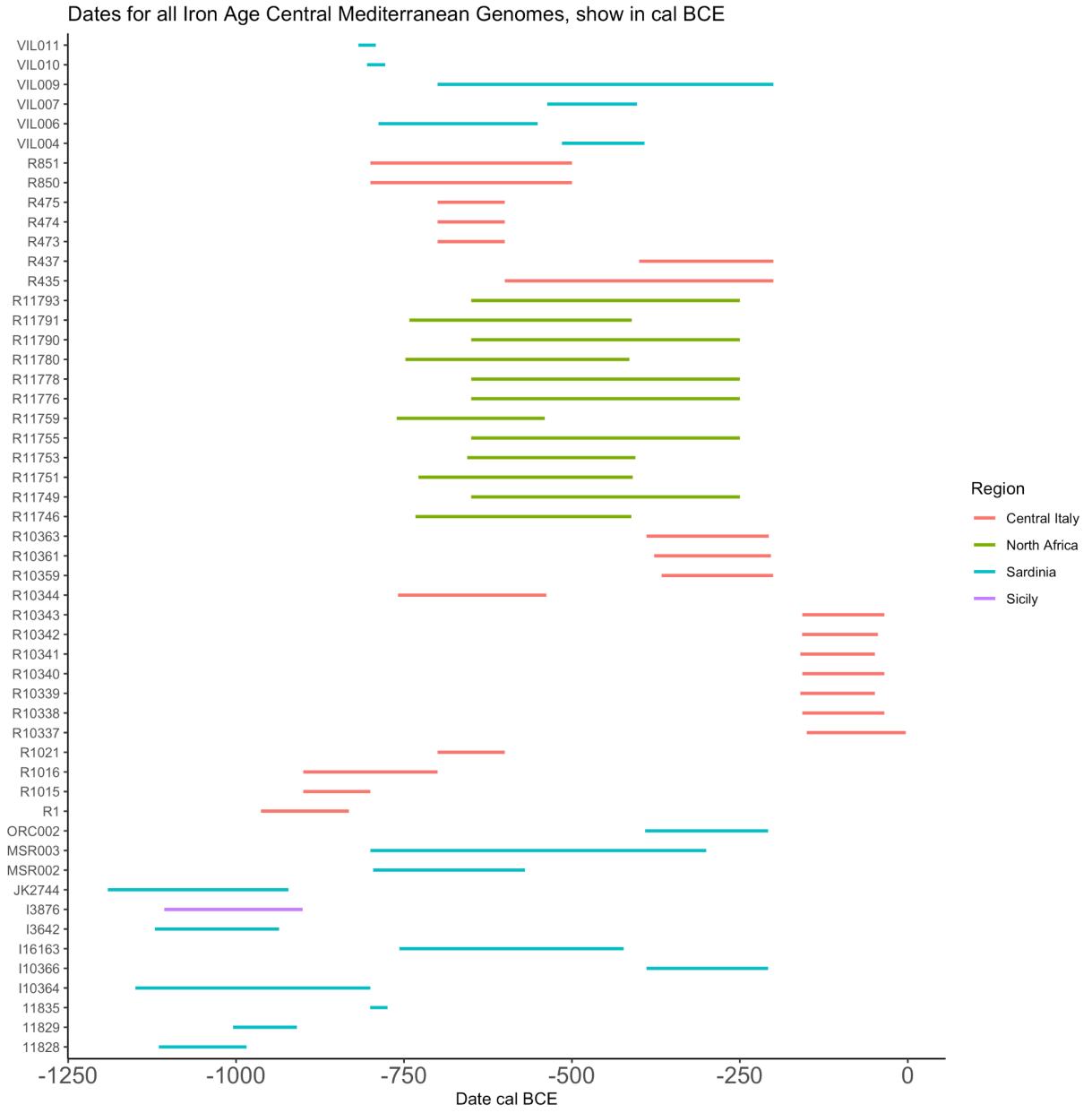

Fig. S1. Timeline of all data from the Iron Age central Mediterranean
This includes new data, plus data from (17, 30, 32). Dates shown are based on radiocarbon dates when available, and otherwise on archaeological date estimates (see Datasets S1, S2, S3).

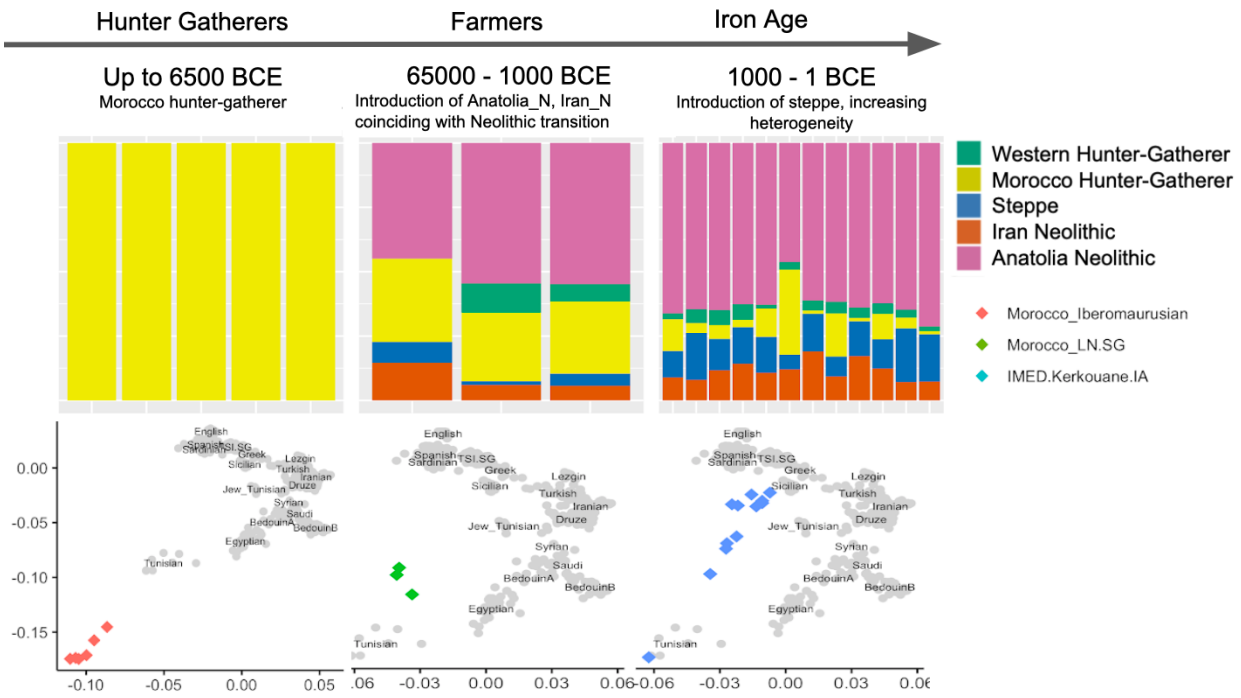

Fig. S2. Maghreb ADMIXTURE and PCA time series

A time series of new and published ancient genomes from North Africa, analyzed using ADMIXTURE and PCA. All new genomes are shown in the Iron Age column. For a larger PCA, see Fig. 3.

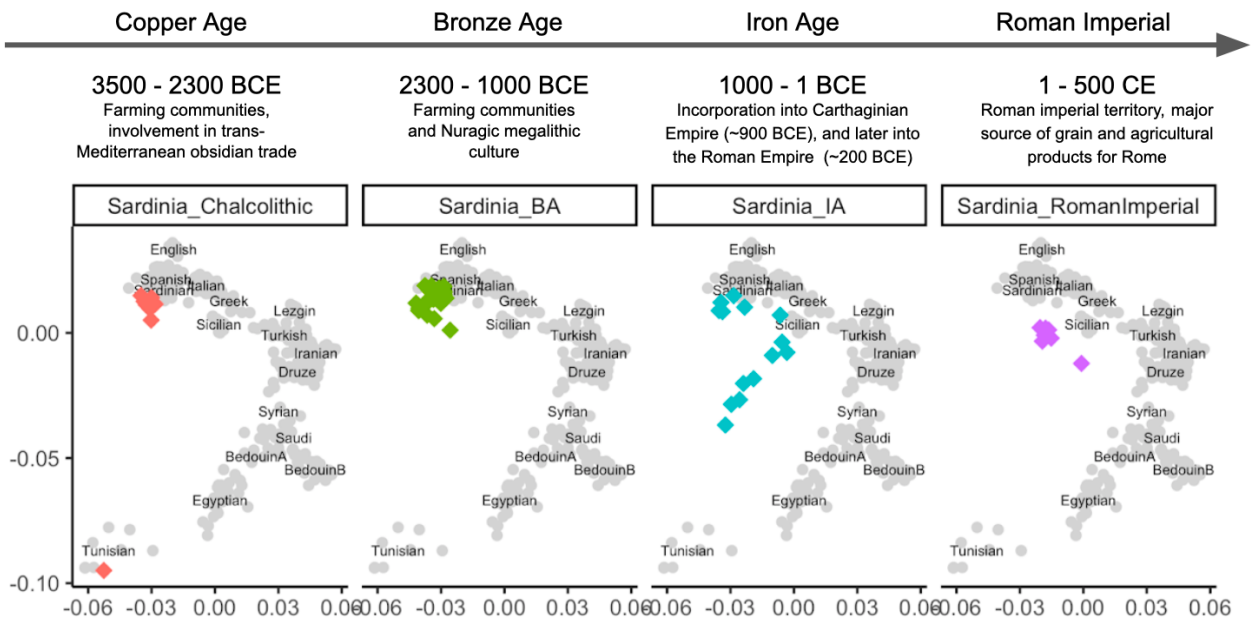

Fig. S3. Sardinia PCA time series

A time series of new and published ancient genomes from Sardinia, analyzed using PCA. This plot shows relatively homogeneous ancestry in the Chalcolithic and Bronze Age, followed by a shift toward North African ancestry in the Iron Age (when the island was part of the Carthaginian Empire) and towards mainland Italy, Sicily and Greece in the Imperial Period (when Sardinia was part of the Roman Empire). These shifts seem to mirror the geopolitical affiliations of Sardinia. All new genomes are shown in the Iron Age column. For a larger PCA, see Fig. 3.

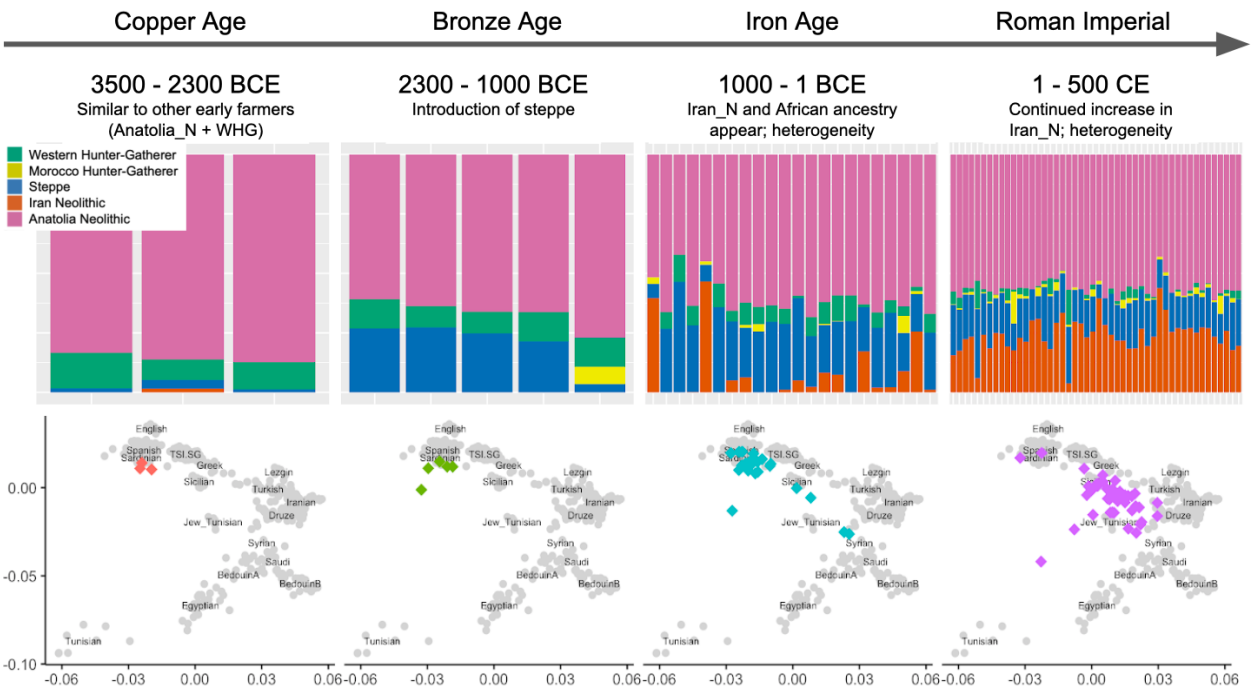

Fig. S4. Central Italy ADMIXTURE and PCA time series
Unsupervised ADMIXTURE plot of genetic data from central Italian individuals organized chronologically.

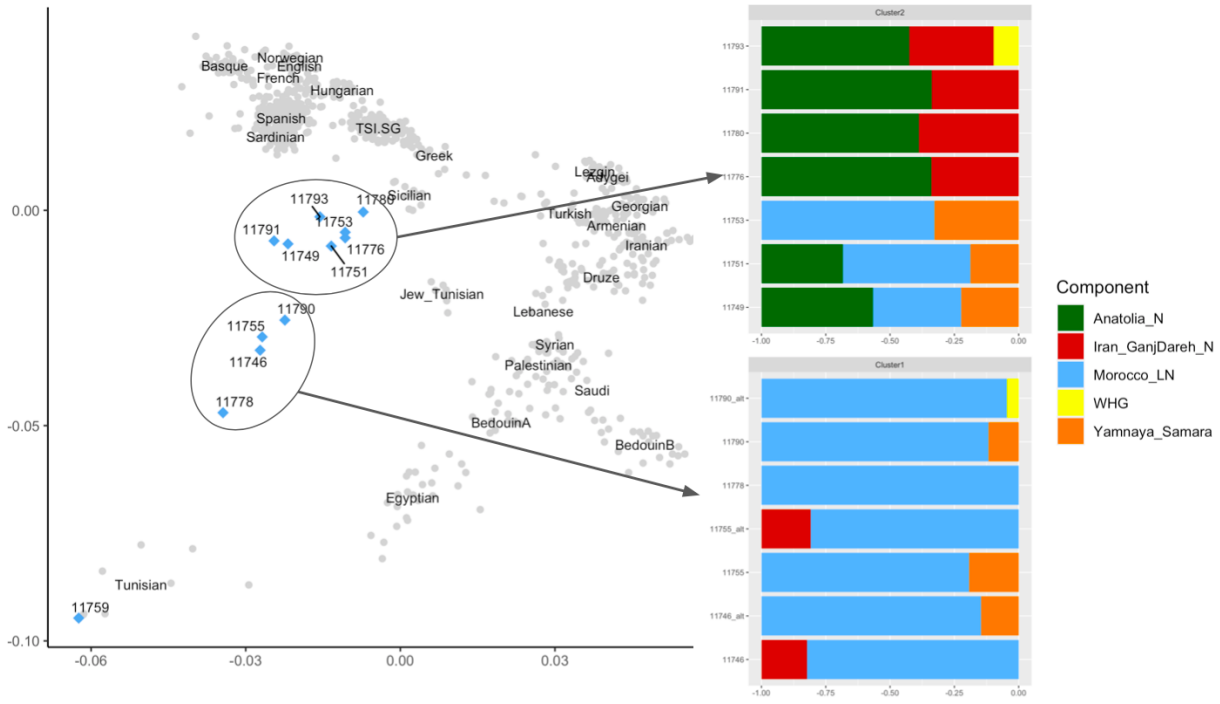

Fig. S5. Kerkouane PCA and qpAdm admixture modeling
Kerkouane PCA and qpAdm admixture modeling.

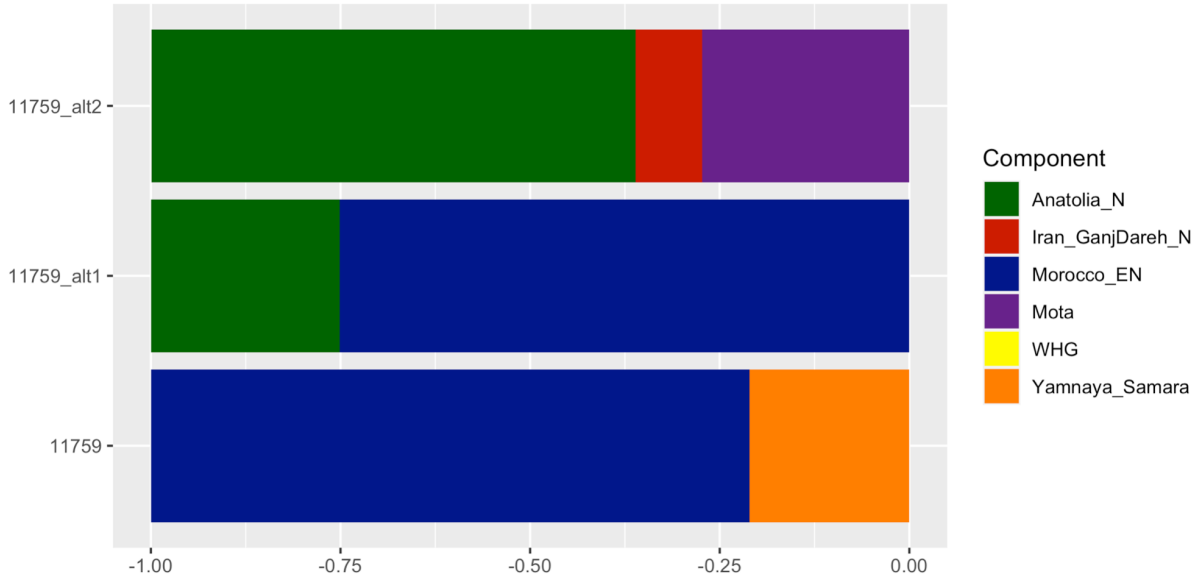

Fig. S6. Admixture modeling for R11759 (Kerkouane Outlier)
11759 is the outlier individual that projects in PCA onto modern Tunisian individuals. There are no working models for this individual with either Morocco_LN or Morocco_Iberomaurusian, but using either Morocco_EN or Mota (a 4500BP individual from Ethiopia) as sources produce working models, all of which are shown above.

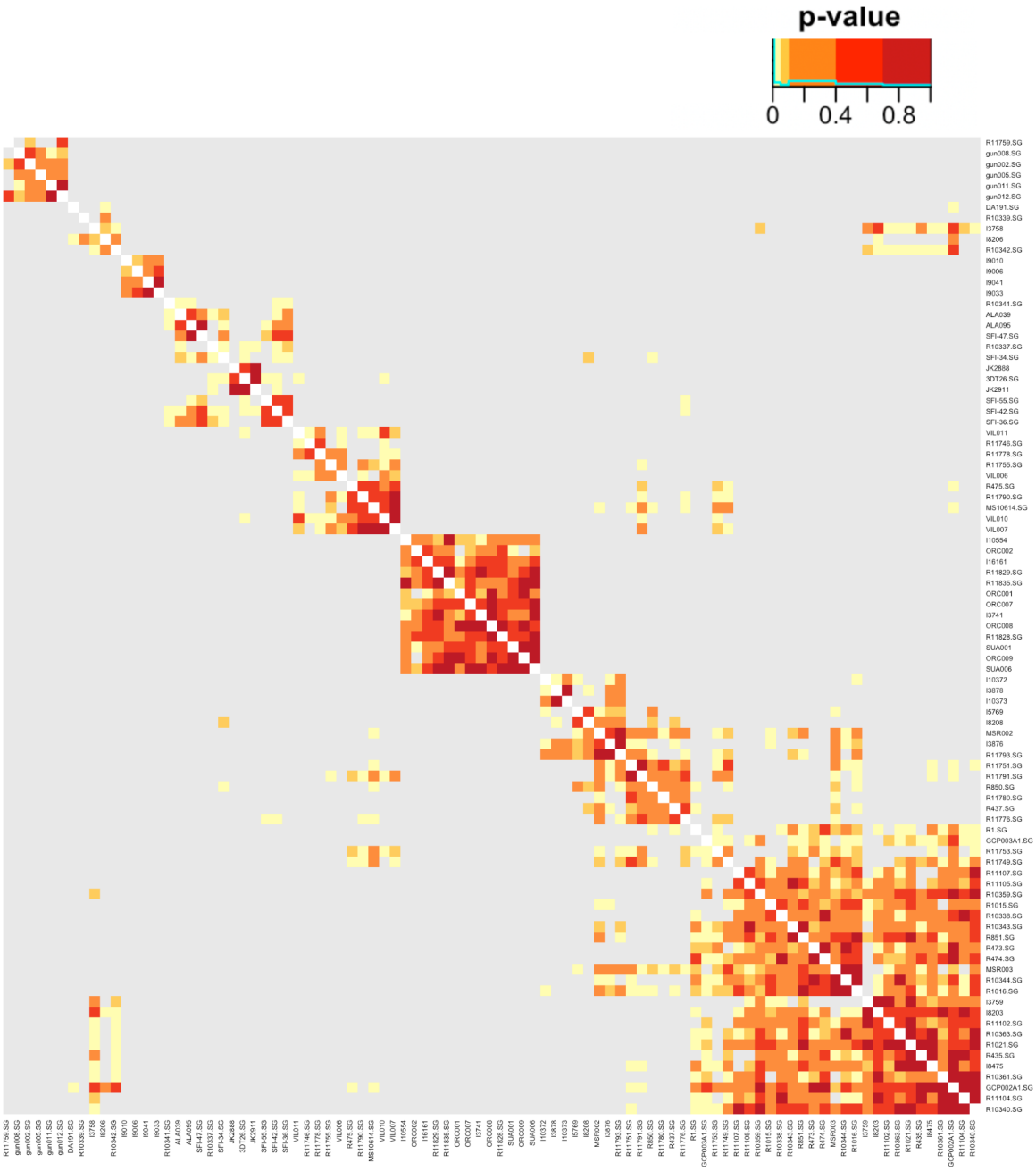

Fig. S7. qpWave heatmap with individuals labels

qpWave heatmap shown in Fig 5, with individual IDs included as labels. The plot shows the clustering of Bronze Age and Iron Age genomes from the central Mediterranean with other relevant ancient individuals. Heatmap colors represent the p-values for each pair-wise model. Values over 0.01 (shown in yellow) indicate that a pair of individuals can be modeled with the same ancestry components in qpAdm in comparison to a set of reference populations (Mbuti.DG, Russia_Ust_Ishim.DG, CHG, Russia_EHG, Iberia_ElMiron, Czech_Vestonice1, Russia_MA1_HG.SG, Israel_Natufian, Jordan_PPNB, Western Hunter-Gatherer (WHG), Yamnaya Samara, Anatolian Neolithic, Iranian Neolithic, and Late Neolithic farmers from Morocco).

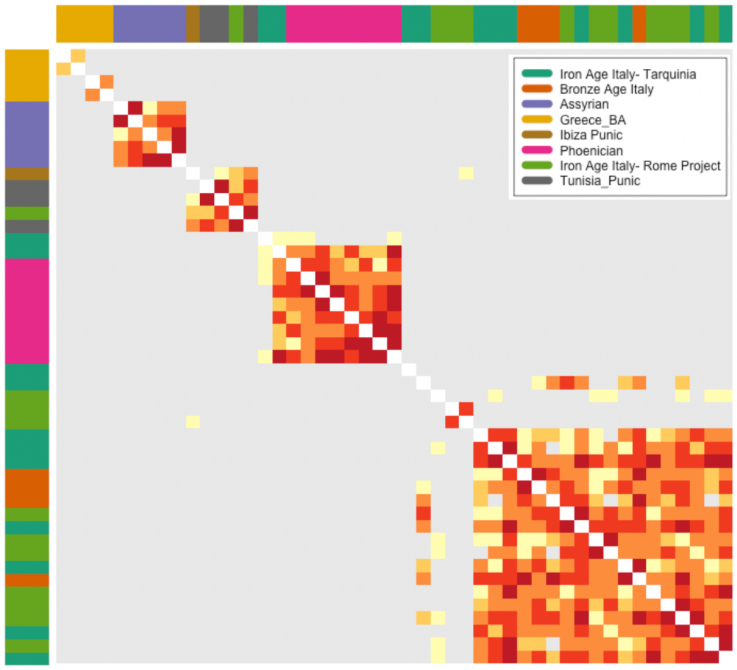

Fig. S8. qpWave analysis focused on central Italy
Localized qpWave analysis, focusing on the Italian Bronze and Iron Age individuals.

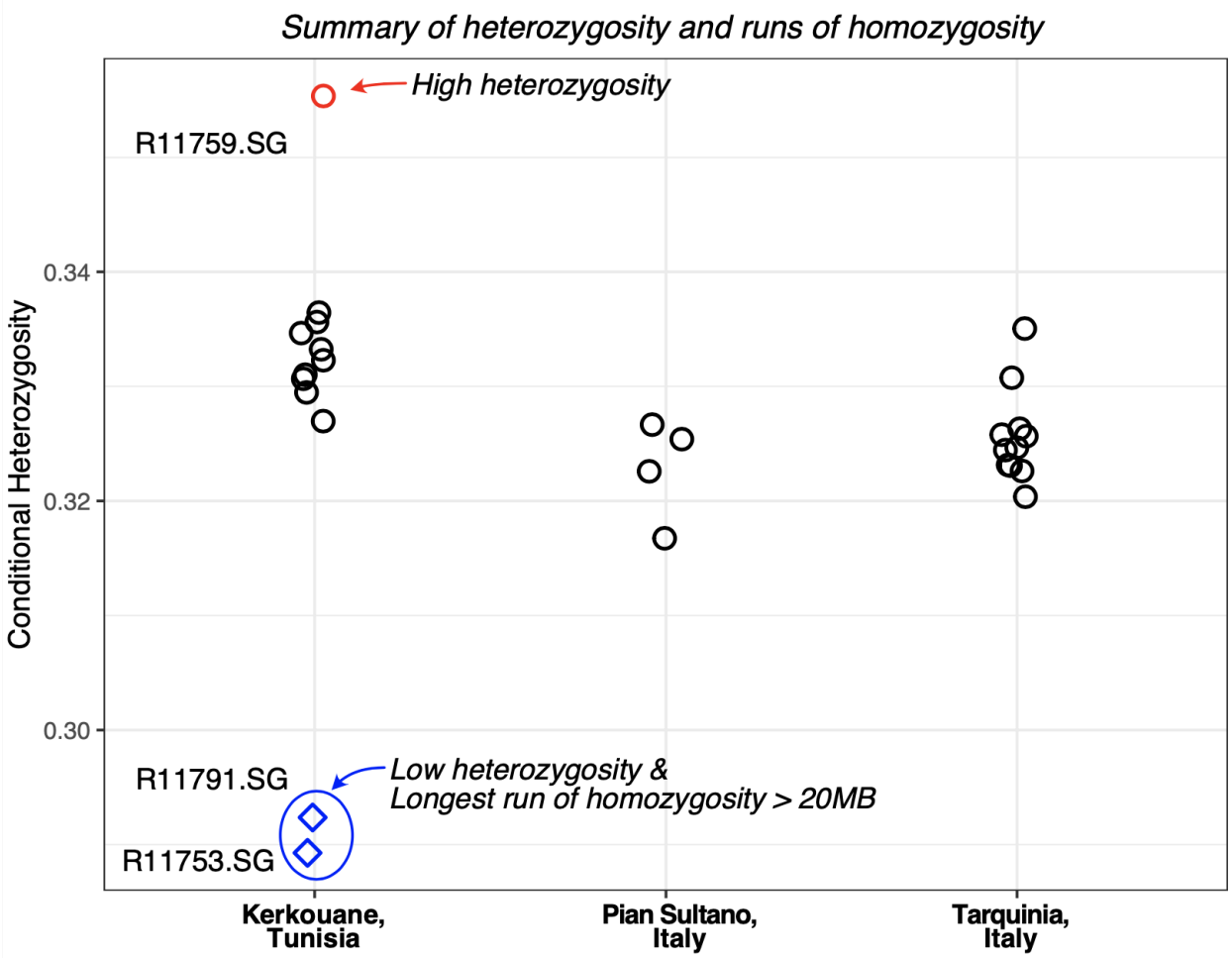

Fig. S9. Conditional Heterozygosity
We calculated heterozygosity using variants that are already known to be segregating in human populations, following the same approach as in (17).

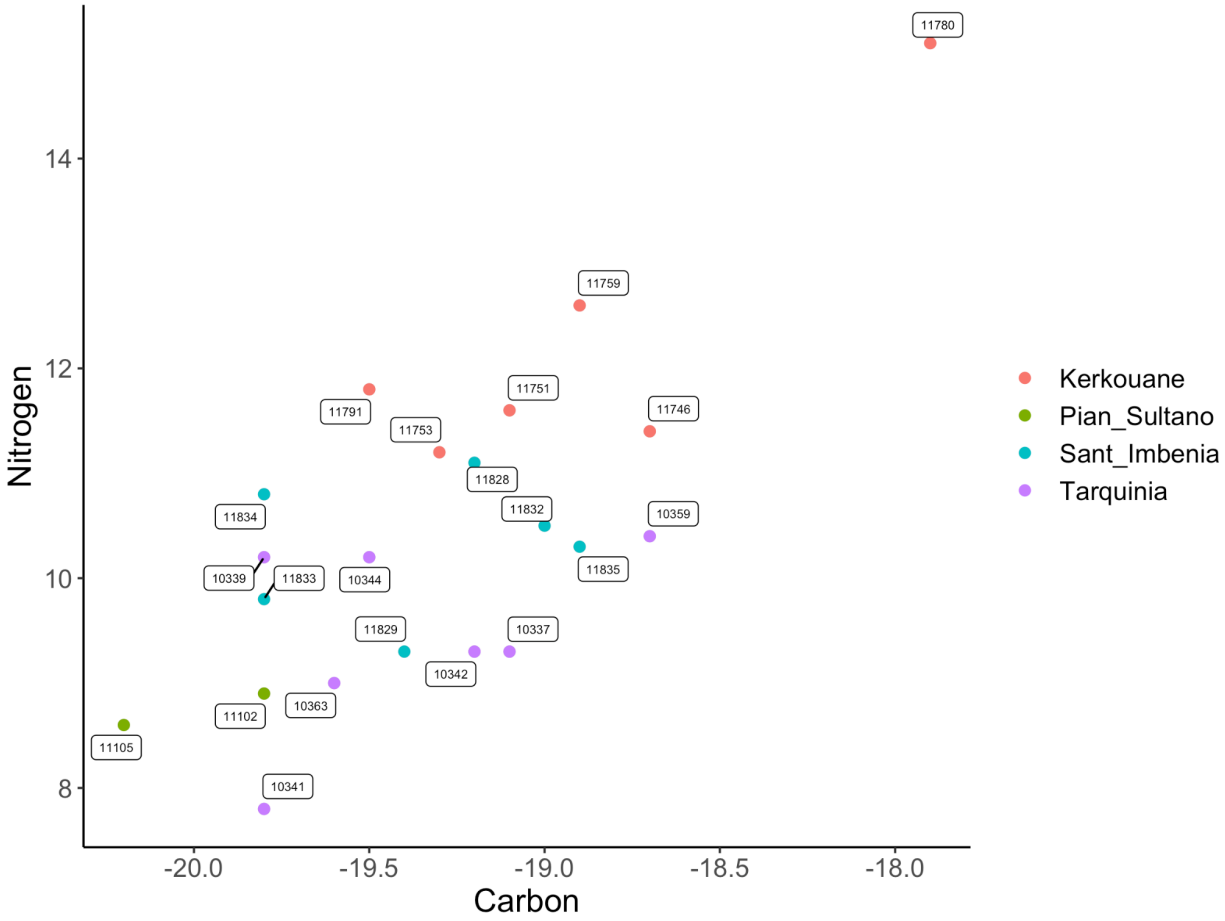

Fig. S10. Combined dietary isotopes across all sites
Combined Dietary Isotopes for individuals across all sites studied.

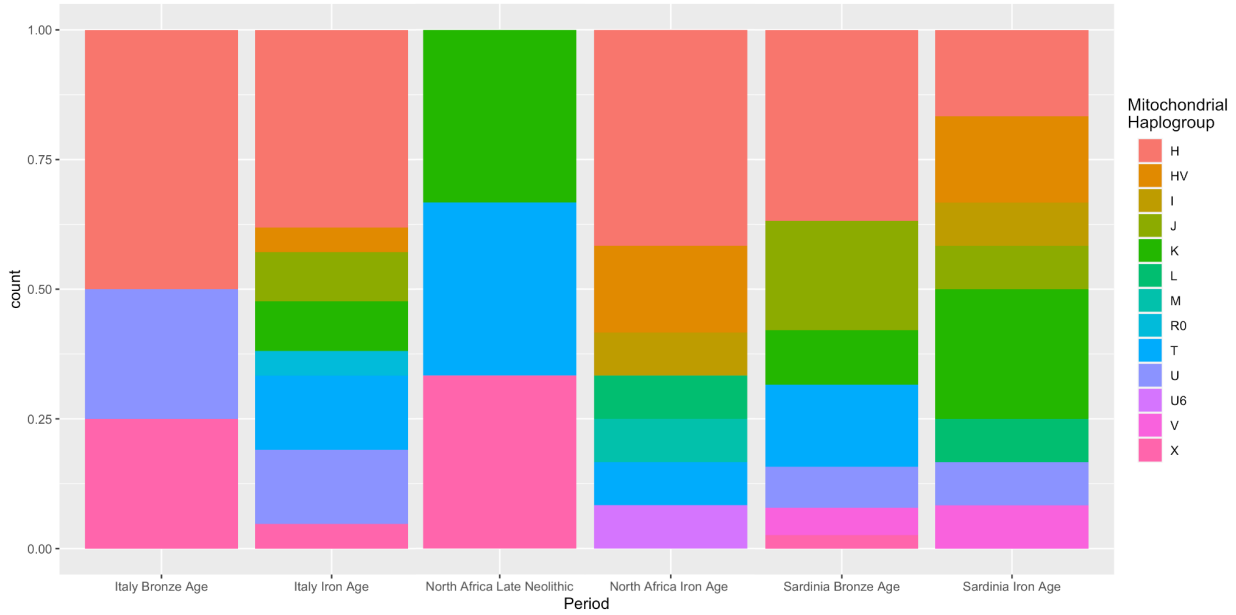

Fig. S11. Mitochondrial haplogroups

Mitochondrial haplogroups for each region in the Iron Age Central Mediterranean and the preceding period, show in percent of population.

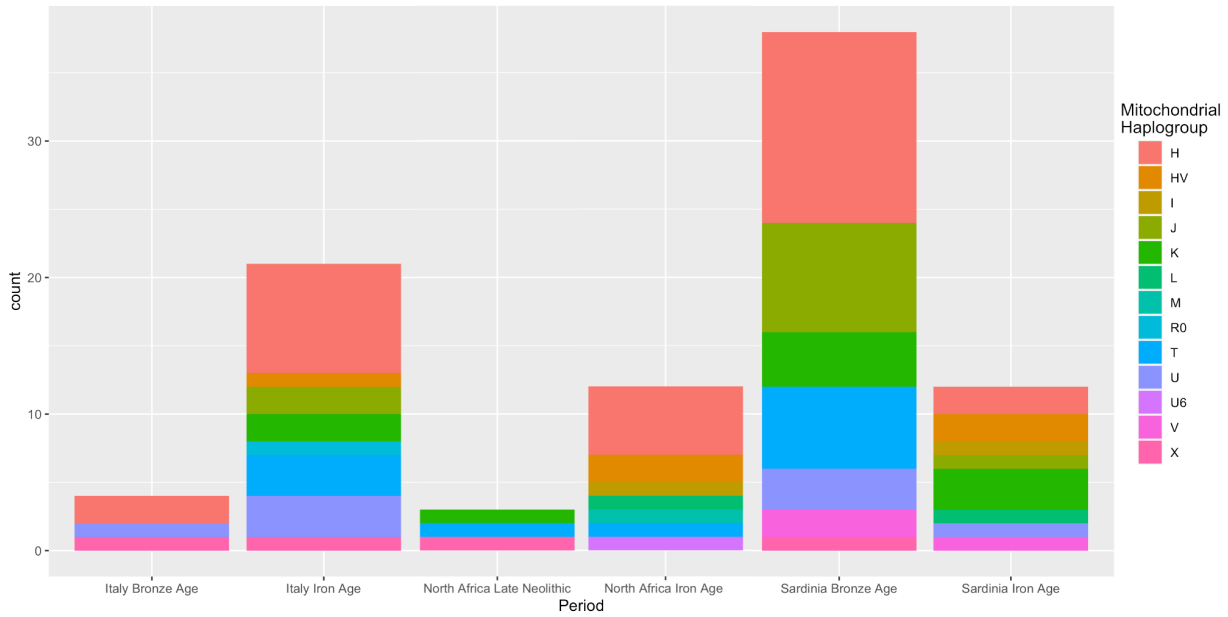

Fig. S12. Mitochondrial haplogroups in absolute counts
Mitochondrial haplogroups for each region in the Iron Age Central Mediterranean and the preceding period, shown in absolute counts.

Fig. S13. Tomb of the Leopards at Tarquinia

One of the painted tombs at Tarquinia, depicting banqueters feasting. This fresco dates to the 5th century BCE. Photograph taken by H. Moots.

Supplementary Tables

Table S1. Burial context and kinship information

Pian Sultano - Italy Bronze Age

ID	qpWave Group	Related?
11102	Bronze Age Italy	
11104	Bronze Age Italy	✔
11105	Bronze Age Italy	✔
11107	Bronze Age Italy	

Kerkouane - Tomb 1

ID	qpWave Group	Related?
11746	Carthaginian	
11749	Sicily/Greece	
11751	Sicily/Greece	

Kerkouane - Tomb 4

ID	qpWave Group	Related?
11776	Sicily/Greece	
11778	Carthaginian	
11780	Sicily/Greece	

Tarquinia- Italy Iron Age

ID	qpWave Group	Related?
10337	Levant	
10338	Bronze Age Italy	
10339	Central Europe/Celtic	
10340	Bronze Age Italy	
10341	Levant	
10342	Central Europe/Celtic	
10343	Bronze Age Italy	

Kerkouane - Tomb 2

ID	qpWave Group	Related?
11753	Sicily/Greece	
11755	Carthaginian	
11759	Saharan	

Kerkouane - Tomb 15

ID	qpWave Group	Related?
11790	Carthaginian	
11791	Sicily/Greece	
11793	Sicily/Greece	

Burial context and kinship information for individuals in this study. Colors show qpWave ancestry groups from Fig. 5.

Table S2. Runs of homozygosity

Sample	Site	Number of ROH segments (>5Mb)	Total length of ROH	Length of longest ROH segment
R11778.SG	Kerkouane	4	23	8.5
R10339.SG	Tarquinia	5	25	6
R11753.SG	Kerkouane	19	424.9	57.2
R11791.SG	Kerkouane	24	391.3	53.6

Summary of homozygosity for individuals with more than one homozygosity segment (>5Mb).

Supplementary Datasets

Dataset S1. Newly reported ancient individuals
Information about the newly reported individual genomes in the study, including sample ID, burial number, dates, latitude, longitude, site, country, genome-wide coverage, SNP coverage, and contamination estimates.

Dataset S2. Ancient individual genomes used in analyses
The IDs and populations categories for previously published ancient genomes used in the study. Each tab in the dataset shows the individuals and populations used for a different set of analyses. Tab 1 shows the individuals used in PCA. Tab 2 shows the individuals used in Admixtools (qpWave and qpAdm) analyses. Tab 3 shows the source populations used in supervised ADMIXTURE analysis.

Dataset S3. AMS dating and isotope analysis results
AMS dating and carbon and nitrogen isotopic results for the newly reported individuals in this study.

SI References

1. M. H. Fantar, L'urbanisme et l'architecture puniques: le cas de Kerkouane. *Fenicios y territorio: actas del II Seminario* (2000).

2. H. Fantar, Le cavalier marin de Kerkouane. *Africa* **1**, 19–32 (1988).

3. M. H. Fantar, Kerkouane: une cité punique au Cap-Bon (1987).

4. R. Miles, *Carthage must be destroyed: the rise and fall of an ancient Mediterranean civilization* (Allen Lane, 2010).

5. M. Fantar, Espaces culturels à Kerkouane. *Comptes rendus des séances de l'Académie des Inscriptions et Belles-Lettres* **147**, 817–824 (2003).

6. F. Trucco, C. Iaia, D. De Angelis, La necropoli di Villa Bruschi Falgari di Tarquinia. *Le comunità della preistoria italiana. Studi e ricerche sul Neolitico e le età dei Metalli in memoria di Luigi Bernabò Brea*, 407–416 (2003).

7. G. B. Gianni, A. Garzulino, S. Kay, M. Marzullo, C. Smith, CIVITA DI TARQUINIA (COMUNE DI TARQUINIA, PROVINCIA DI VITERBO, REGIONE LAZIO). *Papers of the British School at Rome* **86**, 328–332 (2018).

8. G. Bagnasco Gianni, M. Marzullo, A. Garzulino, Scavo e scuola a Tarquinia. Internazionalizzazione e formazione a difesa della fragilità di un sito UNESCO in *G. Bagnasco Gianni, S. Bortolotto, A. Garzulino, M. Marzullo, Milano Internazionale: La Fragilità Territoriale Dei Contesti Archeologici, Atti Del Convegno Internazionale (Milano, 13 Marzo 2019)*, (All'Insegna del Giglio, 2020), pp. 11–15.

9. F. Vermeulen, "Roman colonisation and early urbanisation" in *Revealing a Roman Landscape. Potentia and the Potenza Valley between the Apennines and the Adriatic Sea*, (Ante Quem, 2017), pp. 26–28.

10. K. P. Freund, A long-term perspective on the exploitation of Lipari obsidian in central Mediterranean prehistory. *Quat. Int.* **468**, 109–120 (2018).

11. R. Pinhasi, D. M. Fernandes, K. Sirak, O. Cheronet, Isolating the human cochlea to generate bone powder for ancient DNA analysis. *Nat. Protoc.* **14**, 1194–1205 (2019).

12. R. Pinhasi, *et al.*, Optimal Ancient DNA Yields from the Inner Ear Part of the Human Petrous Bone. *PLoS One* **10**, e0129102 (2015).

13. N. Rohland, M. Hofreiter, Ancient DNA extraction from bones and teeth. *Nat. Protoc.* **2**, 1756–1762 (2007).

14. J. Dabney, *et al.*, Complete mitochondrial genome sequence of a Middle Pleistocene cave bear reconstructed from ultrashort DNA fragments. *Proc. Natl. Acad. Sci. U. S. A.* **110**, 15758–15763 (2013).

15. M. Meyer, M. Kircher, Illumina sequencing library preparation for highly multiplexed target capture and sequencing. *Cold Spring Harb. Protoc.* **2010** (2010).

16. G. Renaud, V. Slon, A. T. Duggan, J. Kelso, Schmutzi: estimation of contamination and

endogenous mitochondrial consensus calling for ancient DNA. *Genome Biol.* **16**, 224 (2015).

17. M. L. Antonio, *et al.*, Ancient Rome: A genetic crossroads of Europe and the Mediterranean. *Science* **366**, 708–714 (2019).

18. M. Martin, Cutadapt removes adapter sequences from high-throughput sequencing reads. *EMBnet.journal* **17**, 10 (2011).

19. H. Li, R. Durbin, Fast and accurate short read alignment with Burrows-Wheeler transform. *Bioinformatics* **25**, 1754–1760 (2009).

20. H. Li, *et al.*, The Sequence Alignment/Map format and SAMtools. *Bioinformatics* **25**, 2078–2079 (2009).

21. H. Jónsson, A. Ginolhac, M. Schubert, P. L. F. Johnson, L. Orlando, mapDamage2.0: fast approximate Bayesian estimates of ancient DNA damage parameters. *Bioinformatics* **29**, 1682–1684 (2013).

22. T. S. Korneliussen, A. Albrechtsen, R. Nielsen, ANGSD: Analysis of Next Generation Sequencing Data. *BMC Bioinformatics* **15**, 356 (2014).

23. I. Lazaridis, *et al.*, Ancient human genomes suggest three ancestral populations for present-day Europeans. *Nature* **513**, 409–413 (2014).

24. H. Weissensteiner, *et al.*, HaploGrep 2: mitochondrial haplogroup classification in the era of high-throughput sequencing. *Nucleic Acids Res.* **44**, W5–W63 (2016).

25. M. Kuhn, J. Manuel, M. Jakobsson, T. Günther, Estimating genetic kin relationships in prehistoric populations. *PLoS One* **13**, e0195491 (2018).

26. V. Hunter, S. B. Pomeroy, Families in Classical and Hellenistic Greece: Representations and Realities. *Phoenix* **52**, 395 (1998).

27. N. Patterson, A. L. Price, D. Reich, Population structure and eigenanalysis. *PLoS Genet.* **2**, e190 (2006).

28. R. Maier, *admixtools* (Github) (January 18, 2022).

29. I. Olalde, *et al.*, The genomic history of the Iberian Peninsula over the past 8000 years. *Science* **363**, 1230–1234 (2019).

30. D. M. Fernandes, *et al.*, The spread of steppe and Iranian-related ancestry in the islands of the western Mediterranean. *Nat Ecol Evol* **4**, 334–345 (2020).

31. D. H. Alexander, J. Novembre, K. Lange, Fast model-based estimation of ancestry in unrelated individuals. *Genome Res.* **19**, 1655–1664 (2009).

32. J. H. Marcus, *et al.*, Genetic history from the Middle Neolithic to present on the Mediterranean island of Sardinia. *Nat. Commun.* **11**, 939 (2020).